# A Patient-Mounted, Telerobotic Tool for CT-Guided Percutaneous Interventions

**Conor J. Walsh**
**Nevan C. Hanumara**
**Alexander H. Slocum**

Department of Mechanical Engineering,
Massachusetts Institute of Technology,
Cambridge, MA 02139

**Jo-Anne Shepard**
**Rajiv Gupta**

Department of Radiology,
Massachusetts General Hospital,
Boston, MA 02114

*This paper describes Robopsy, an economical, patient-mounted, telerobotic, needle guidance and insertion system, that enables faster, more accurate targeting during CT-guided biopsies and other percutaneous interventions. The current state of the art imaging technology facilitates precise location of sites within the body; however, there is no mechanical equivalent to then facilitate precise targeting. The lightweight, disposable actuator unit, which affixes directly to the patient, is composed primarily of inexpensive, injection molded, radiolucent, plastic parts that snap together, whereas the four micromotors and control electronics are retained and reused. By attaching to a patient, via an adhesive pad and optional strap points, the device moves passively with patient motion and is thus inherently safe. The device's mechanism tilts the needle to a two degree-of-freedom compound angle, toward the patient's head or feet (in and out of the scanner bore) and left or right with respect to the CT slice, via two motor-actuated concentric, crossed, and partially nested hoops. A carriage rides in the hoops and interfaces with the needle via a two degree-of-freedom friction drive that both grips the needle and inserts it. This is accomplished by two rubber rollers, one passive and one driven, that grip the needle via a rack and pinion drive. Gripping is doctor controlled; thus when not actively being manipulated, the needle is released and allowed to oscillate within a defined region so as to minimize tissue laceration due to the patient breathing. Compared to many other small robots intended for medical applications, Robopsy is an order of magnitude less costly and lighter while offering appropriate functionality to improve patient care and procedural efficiency. This demonstrates the feasibility of developing cost-effective disposable medical robots, which could enable their more widespread application.*
[DOI: 10.1115/1.2902854]

*Keywords: medical, patient-mounted, robotics, disposable, spherical mechanism, image-guided, computed tomography, percutaneous interventions, biopsy*

## 1 Introduction

Minimally invasive, image-guided interventional radiological procedures typically entail insertion of an instrument through a small incision and its subsequent dexterous manipulation while viewing fluoroscopic, computed tomography (CT), ultrasound, or magnetic resonance (MR) images. Examples of such interventions include image-guided percutaneous biopsies, drainages, radio frequency (RF) ablations, drug deliveries, and brachytheraphy seed implantations. In current clinical practice, insertion and manipulation of these instruments are typically done manually. This paper discusses the design and development of a new tool to assist in percutaneous (through the skin) CT-guided pulmonary interventions and demonstrates a cost-effective model for medical robotics.

Lung cancer is the most deadly cancer in the US, with 213,380 persons diagnosed in 2006 and an average five-year survival rate of only 15.5% [1]. Earlier detection is essential to improving patient prognosis, as demonstrated by a recent study where CT screening was conducted of 31,567 at-risk subjects. For those subsequently diagnosed with Stage I lung cancer whom underwent surgical resection within one month, the survival rate was 92% [2].

The estimated 125,000 percutaneous biopsy procedures performed per annum in the United States are unnecessarily difficult, even for an experienced practitioner, because while current technology allows lesions to be precisely *located*, they cannot yet be precisely *targeted*. A CT scanner is capable of providing high-resolution (submillimeter) images, enabling a radiologist to confirm the presence of a suspect lesion and determine its size, precise location, and extent of encroachment on nearby tissue and organs. However, diagnosing the lesion requires conducting a biopsy to obtain a tissue sample for histological analysis. In contrast to the actual scanning, the current percutaneous biopsy procedure is manual, iterative, and consequently imprecise and time consuming.

**1.1 Percutaneous Biopsy Procedure.** The procedure begins with a broad localization CT scan of the thorax, with slices spaced at 5 mm followed by a more detailed scan, with 2.5 mm spaced slices, of the region of interest. A radio-opaque positioning grid is then adhered to the patient and the gantry may be tilted so as to provide a clear plane, free of ribs or other structures that need to be avoided. From this initial scan, the radiologist identifies the lesion's position and precisely plans the needle's insertion trajectory in terms of angles and depth from the selected insertion point on the grid. Then considering these measurements, he/she leaves the control room, slides the patient out of the CT scanner bore, locates the insertion point via the grid, and manually begins inserting the needle, with minimal visual guidance. This process is iterative: The radiologist alternates between control scans, to determine the location of the needle tip with respect to the target, and needle manipulations, to orient and advance the needle towards the target. Each cycle necessitates sliding the patient in and

Manuscript received September 26, 2007; final manuscript received February 7, 2008; published online April 8, 2008. Review conducted by Gerald E. Miller. Paper presented at the ASME 2005 Design Engineering Technical Conferences and Computers and Information in Engineering Conference (DETC2005), Long Beach, CA, September 24–28, 2005.

out of the scanner bore and the medical team shuttling back and forth between the scanner chamber and radiation shielded control room. During insertion, the goal is to grip the needle firmly for only a moment while advancing it briskly. The insertion procedure may consume up to 1 h of scanner time and overall the biopsy procedure may take 2 h, especially when samples are acquired from multiple sites within the lesion, requiring postinsertion needle adjustment. The procedure is often stressful and fatiguing for radiologists, due to the difficulty in accurately placing the needle while avoiding surrounding structures, and tiresome and uncomfortable for the patients who may be only mildly sedated. Using the standard manual method, lesions smaller than 10 mm cannot be reliably targeted, and the overall successful sample acquisition rate is only 77% [3]. In addition, it is not possible to reliably target specific portions of a lesion, such as those that have been shown to be metabolically active on a positron emission tomography (PET) scan. Furthermore, multiple needle manipulations performed after the needle has crossed the lung's pleurae (covering membranes) increase the risk of pneumothorax (partial or full lung collapse). Results and complication rates vary widely with physician training and skill, with interventional radiologists who have not been trained in thoracic interventions find the procedure more challenging.

Some practitioners do attempt to biopsy subcentimeter lesions but tissue yield plummets as lesion size decreases [3]; for lesions between 5 and 10 mm in diameter, the accuracy is 52%, and for lesions less than 5 mm, the manual biopsies are often inadequate. Considering a 1 cm lesion at a 10 cm depth, if the practitioner is aiming at the center, an angular error of only 3 deg will result in a missed lesion. Subcentimeter lesions may also significantly require more needle passes, thus increasing the risk of pneumothorax. Instead, most practitioners resort to "watchful waiting" and schedule repeat tri-monthly observational scans, in lieu of a definitive diagnosis. This practice, which can delay treatment, is understandably non-ideal for the patient. Although PET provides an alternative method of diagnosing cancer; it, too, is insensitive to subcentimeter lesions.

There is an increasing trend for more localized treatment of cancerous tumors with brachytherapy and radio frequency (RF) ablation being the most common. Both of these procedures require accurate placement of the probes, as small deviations can create significant areas of over- and underdosage or ablation. Although promising, in clinical practice, the application of these treatments is still infrequent due, in part, to the difficulties in accurately *targeting* the lesions.

**1.2 Alternative Approaches.** A number of other approaches are either commercially available or being developed to assist in CT-guided percutaneous procedures. These include passive laser alignment systems and CT scanner mounted robotic systems, as well as some patient-mounted approaches. The *SimpliCT* (Neorad, Oslo, Norway) consists of a laser mounted on a wheeled stand [4]. Following the normal planning steps, it is positioned over the patient, outside the scanner bore, and the beam set to the correct compound entry angle and aimed at the desired insertion point; then the needle is inserted by hand using the beam as a guide. In a multicenter European trial, a mean of 1.2 needle passes was necessary to reach 65 out of 67 target lesions having a mean diameter of 3.1 cm, of which 24 were located in the lung. A new needle pass was defined as a reinsertion of the needle with a new angle; it is not clear whether further manipulations were needed after initial lesion targeting, nor was comparison made with freehand techniques in the report. The mean deviation of the needle from the planned angular trajectory was 1.8 deg but in four lung biopsy cases the angle difference was 5 deg or more, due to a lack of support for the needle by the lung tissue. The mean targeting time between the initial localizing scan and the needle's confirmation in the target was 15.6 min; the total number of CT scans was not reported. The *PatPos Invent* (LAP of America L.C, FL) performs a similar function, but the laser's gantry is mounted directly to the CT scanner [5]. However, if the lesion is small and in the early phase, when it may be most desirable to biopsy, these systems will be limited in their ability to target subcentimeter lesions as needle insertion is still manual.

A number of groups are pursuing the approach of a robotic manipulator mounted to the scanner bed. One example is the *Innomotion* (Innomedic Inc., Herxheim, Germany) that is mounted on a large frame that extends over the patient, limiting access to the patient. Remotely from the control room, employing MRI and CT compatible pneumatics and an interface integrated with the imaging data, it positions and orients a sterile alignment device under image guidance. Later, with the patient outside the bore, the needle is inserted manually along the guide without real-time feedback from the CT scanner [6].

Another CT scanner bed mounted approach is the *AcuBot* system from The Johns Hopkins University that consists of a combination of the one degree-of-freedom (DOF) radiolucent percutaneous access of the kidney (*PAKY*) needle driver, mounted to the two DOF remote center of motion (*RCM*) system that pivots the needle in two angles, connected to a passive positioning arm, which in turn is positioned by a 3 DOF *X-Y-Z* stage mounted to a bridge structure over the patient [7]. The articulating arm is used to position the PAKY near the desired insertion point and the positioning is fine-tuned with the stage. The needle is then tilted with the RCM and inserted with the PAKY. There does not appear to be any allowance for patient respiration or unexpected motion. In a cadaver study at Georgetown University, 12 metal balls of 1 mm diameter were placed in a lumbar spine from L1 to L4 vertebra and targeted using the PAKY-RCM via an anterior/posterior (A/P) approach and lateral fluoroscopic guidance. The average needle placement error was 1.44 mm with a standard deviation of 0.66 mm [8]. They have recently completed a 20 patient study placing a 22 gauge needle into a preselected spinal target location, under fluoroscopic guidance, to deliver an anesthetic block directly to the source of pain. With half of the patients, the needle insertion followed the standard, iterative manual procedure and for the other half the robot was used. The mean accuracies were comparable at 1.2 mm and 1.1 mm, respectively, as was the patient perceived pain reduction postprocedure. This robotic needle driver has also been shown to enable a radiologist to target a lesion in a custom-designed respiratory motion lung phantom under real-time fluoroscopic CT guidance [9]. The respiratory motion of the phantom was paused for 30 s (simulating a breath hold, requested of the patient) while the radiologist commanded the needle toward lesions of unreported size. For the 20 trials that were performed, the mean time to place the needle, after the simulated breath hold, under fluoroscopic CT guidance was 12.1 s and the average dose length product was 92.5 mGy cm. This did not include preliminary scans and setup time. Although this study demonstrates the benefit of robotically assisted needle placement, the system has a large number of DOF and poses a safety risk should inadvertent patient movement occur.

The 7 DOF *CT-BOT*, being developed by a team in Strasburg, straps to a patient and operates within the CT scanner bore to position a needle tip in an *X-Y* plane, tilt the needle in two angles and insert while spinning it [10]. This system weighs approximately 3 kg, employs ultrasonic motors with encoders coupled to harmonic drives, and grips the needle firmly throughout the procedure. They are developing a haptic interface and integrating the CT images into an interface for point-and-click targeting capability. The ability of the system to target a lesion under CT-scan guidance was evaluated and a precision of 3 mm was observed for a typical interventional depth of 200–250 mm.

The *Light Puncture Robot* (LPR) being developed in Grenoble is pneumatically actuated and is both CT and MRI compatible. The three DOF effecter orients and inserts a needle without releasing it, weighs 1 kg, and rests upon the patient. It is connected to a surrounding frame by straps that are actuated in order to

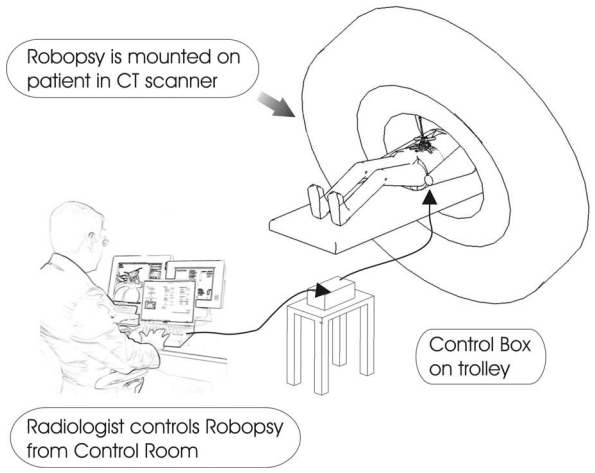


**Fig. 1 The Robopsy system. A disposable, patient-mounted telerobot is controlled by a radiologist in the radiation-shielded control room using a custom interface running on a laptop.**

translate the device [11]. They have a registration method with the CT image. In initial experiments on an idealized flat phantom, constructed from foam rubber, the target point (pixel that was chosen on the screen) was reported to have been reached in all cases with an error less than 2 mm.

Robotic systems also have the potential to assist with more targeted forms of treatment. The *MRBot* is a new robot designed for transperineal percutaneous prostate access [12]. It has three translational and two rotational DOFs and is pneumatically driven using custom-designed MRI compatible actuators. A fully automated MR compatible seed injector is used with the robot for performing low dose prostate brachytherapy under MR imaging [13]. Phantom experiments have been performed to access the robot's ability to place seeds in a firm gel (an ideal setup that minimizes needle deflection during insertion) and achieved a mean placement error (imaging, registration, robot positioning, and seed deployment errors) of less than 1.2 mm for over 60 seeds.

**1.3 Robopsy.** There is a clear opportunity to combine the precision of a robotic system with the precise positional data available from a CT image to more accurately target lesions inside the body, for diagnostic sample acquisition and targeted treatments. Radiologists, desiring better needle location feedback, want to be able to remotely insert a needle as concurrently with imaging as possible while maximizing patient safety. Section 1.2 outlined that various medical robots have been already designed for this purpose. Our approach was to create a system, shown in Fig. 1, which seamlessly integrates with the current procedure by augmenting select manual steps and passively compensating for respiration and patient motion. The result is *Robopsy*, an economical, lightweight, disposable, radiolucent telerobotic tool, which adheres directly to a patient inside a CT scanner bore. Guided by the radiologist in the control room, it remotely grips, orients, and inserts a standard biopsy needle while permitting simultaneous imaging of the needle location.

## 2 Defining Device Specifications

The design of Robopsy was based on a careful study of the current percutaneous lung biopsy procedure; however, throughout the design process, it has been intended to address the more general probe insertion problem. A systematic approach was taken whereby each step of the current procedure was analyzed to determine whether or not it was being satisfactorily conducted. Then a partitioning of the tasks between the interventionalist and the telerobot was performed so as to minimize the DOFs that the manipulator had to control. This analysis was essential in understanding the current challenges and in determining timing and accuracy benchmarks to be improved upon in future trials. Data were obtained through discussions with trained interventional radiologists and bench level experiments.

**2.1 Stepwise Decomposition and Task Partitioning.** Our initial analysis identified seven DOFs that the telerobotic manipulator needed to actuate: (1) and (2) $X$ and $Y$ locations of the needle tip with respect to the skin surface prior to insertion, (3) and (4) two angular tilts of the needle, (5) insertion of the needle, (6) rotation of the needle around its long axis, and (7) the ability to selectively grip and release the needle. However, a seven DOF device would require significant complexity, so each DOF was considered with respect to its absolute necessity and whether it could be performed more expediently by the interventionalist than the robot. The first two DOFs to be eliminated from the robot's design specifications were remote $X$ and $Y$ translations as these are infrequently performed by the radiologist once the actual insertion point is selected and marked upon the patient, with the aid of the positioning grid and the CT machine's lasers. Then, after a sterile preparation of the area, the skin at the selected insertion site is nicked and the needle placed just through this nick. Small $X$-$Y$ changes may be effected later, but are not necessarily critical and are relegated to the human operator if ever needed. Axial needle rotation, or twisting, during insertion was found to be less than necessary; it is primarily effected to better secure the need at the desired angle in certain tissue types, but since needle alignment is a primary function of the Robopsy device, needle twisting was seen to be superfluous.

The remaining four "minimal essential DOFs"—two angles for needle orientation, selective gripping of the needle, and needle insertion/retraction—were used to design the current telerobotic manipulator for lung biopsies. The range of motion required for needle angulation was determined, through observing biopsy procedures and meetings with practitioners, to be 30 deg, which is greater than the maximum gantry tilt for most CT scanners. In general, it is desirable to insert the needle as perpendicular to the pleural surface as possible so as to minimize tearing and to pierce the tissue in a predictable manner; however, some tilt in one or both directions may be required, in order to navigate around internal structures, such as ribs and blood vessels and coincide with gantry tilt.

**2.2 Accommodating Patient Motion.** As the biopsy needle is being inserted, two types of motion have to be compensated for in order to ensure patient safety. The first is the vertical motion of the patient's chest due to the respiration. If the biopsy needle were held by a robotic arm attached to the gantry, patient table, or the floor, then in order to compensate for the respiratory motion it would be necessary to employ closed loop control to actively sense chest motion and move the arm accordingly so that the needle retained its position relative to the patient. Furthermore, there would be a risk of significant injury if the patient execute a gross and unpredictable movement, such as sitting up, while the needle was held in the chest. This procedure is usually carried out with either local anesthetic or mild sedation, so undesirable patient motion is a real risk. To mitigate this risk in the simplest way possible, the device was designed to mount directly to the patient so that it would both move up and down with respiratory motion as well as remain attached to and travel with the patient in the case of large motions. By limiting the degrees of freedom, it was possible to produce a robot of sufficiently small scale.

The second motion is oscillation of the needle. As a patient breathes quietly with the biopsy needle inside the lung, the part remaining outside the body is observed to wave (often referred to as waggle) back and forth, describing approximately a 25 deg cone. This motion occurs because the lung's parenchyma, or the respiratory tissue, moves relative to the skin surface. If one were to fix the needle and stop this oscillation, the lung would be lac-

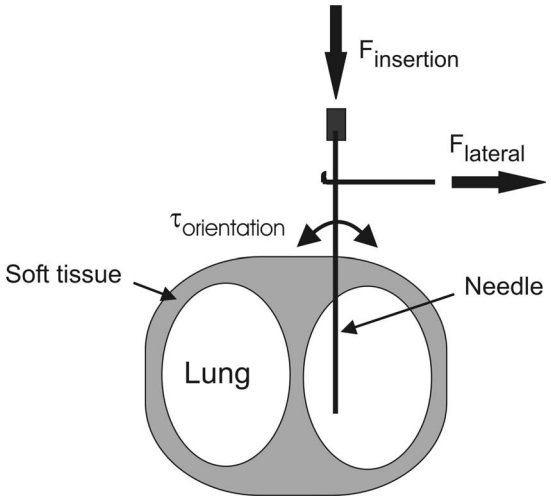


**Fig. 2 Needle insertion experiments. The force to insert a biopsy needle into soft tissue, $F_{insertion}$, and the torque to orientate (tilt) a needle $\tau_{orientation}$ in soft tissue were measured.**

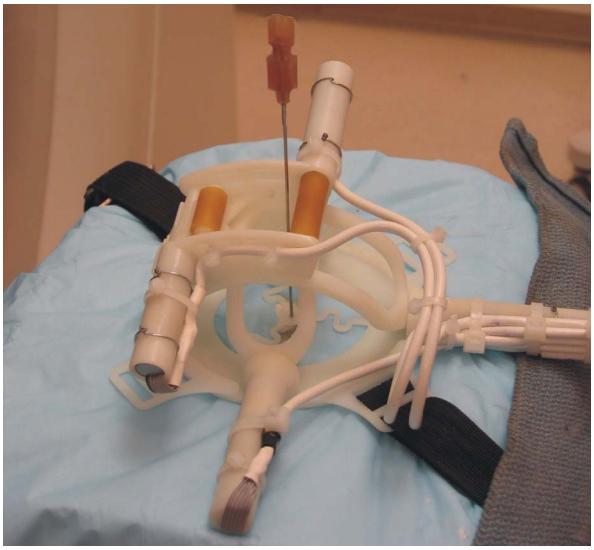

**Fig. 3 Beta prototype. The disposable actuator is shown strapped to a thoracic phantom. The needle is not gripped by the device and is free to move.**

erated by the needle. This led to an important functional requirement for the telerobotic actuator module: It must allow the needle to freely waggle. Thus, once the needle has traversed the pleura, the device must be capable of only firmly gripping the needle for long enough to orient or insert it, after which it must be promptly released. Therefore, Robopsy incorporates a special discretionary needle gripping feature to accomplish this task.

**2.3 Patient-Mounted, CT-Compatible Structure.** A typical CT bore is 70 cm in diameter and the space between the top of an average patient and the bore is approximately 30 cm; this envelope put a constraint on the size of the device as well as the need for a base small enough to mount stably on the curved surface of the patient. Furthermore, it was deemed critical that the device did not restrict immediate access to the patient. In other words, it needed to be easily and quickly placed and removed by a radiologist at any moment during the procedure. An ancillary advantage of a small device, which grips the needle close to the skin surface, is that standard length, or just slightly longer, needles can be used.

Artifacts can strongly distort CT images to the point that they are diagnostically unusable by the radiologist [14]. Metal artifacts were of particular concern in the design of Robopsy. The biopsy needle is metallic and the linear artifact, which it generates, projecting from the tip along its axis, provides a guide for the radiologist to aim toward the target lesion. However, any other metallic elements in the device could distort the image and obscure the desirable needle artifact. Thus the device needed to be designed for construction of primarily radiolucent plastic, which could be visualized but would not distort the CT images. Construction from plastic enabled the device to be designed for injection molding, which coincided with the desire for simplicity, lightweight and low cost. Metallic elements (e.g., motors) were necessary, but they were sufficiently placed outside of the scan plane encompassing the needle so as not to cause image distortion.

**2.4 Needle Insertion and Manipulation.** In order to correctly size the actuators, it was necessary to determine the force required for needle insertion through the skin, muscle, and soft tissue. Okamura et al. performed an experiment where they used a robot arm to insert a needle into bovine liver and recorded the resulting force using a load cell attached to the needle [15]. Their force-displacement data showed a peak of approximately 3.5 N and were characterized by multiple peaks in the force followed by sharp drops, corresponding with the needle puncturing various distinct tissue layers. In order to verify these data, we performed our own bench level experiments, illustrated in Fig. 2, where we measured the force required to insert a standard 19 gauge (0.912 mm) lung biopsy needle into a deceased turkey. From this, we estimated the maximum likely force required for insertion through the chest wall and into the lung to be approximately 4 N. Discussion with doctors at MGH revealed the opinion that a higher force may be needed for some applications. Therefore, a needle insertion force of about 10 N was used as the design specification.

In order to determine the torque required to orientate a needle when it is inserted into a patient, an experiment was performed where a 19 gauge needle was placed at three different depths (10 mm, 50 mm, and 100 mm) into the deceased turkey and the torque required to orientate the needle by 30 deg was recorded. As expected, we found that there was a small resistance to needle manipulation when it was just inserted (10 mm) into the tissue. At needle insertion depths of 50 mm and 100 mm, the required torques were 25 N mm and 60 N mm, respectively. Increasing required torque with increasing depth is predictable as the needle motion is resisted by soft tissue in the chest wall and lung.

## 3 Device Design

The design was driven by the four specified DOFs, identified by studying the current procedure, with the initial constraints of lightweight, patient mounting, and disposability. The beta prototype is shown in Fig. 3.

**3.1 Mechanism Design.** Spherical mechanisms are widely used in many robotic and positioning systems where an arm or instrument is orientated in pitch and yaw angles [16–18]. Dien et al. described using two independent slotted spherical yokes, which, when actuated, can position a pin that rides in both hoops so that it described a near complete hemispherical workspace [16]. Stanisic et al. combined two of these "pointing" mechanisms back to back, such that they can serve as a joint, between two intersecting arms, which is capable of producing singularity free motion [17]. A similar spherical mechanism was chosen to describe the needle's two angular DOFs and is shown in Fig. 4. All components share a common central pivot point that is positioned as closely as possible to the preselected needle insertion point. The two compound angles are accomplished by a pair of concentric, nested hoops that are attached to a fixed base, which is mounted to the patient. The axes of the two hoops are coplanar and their intersection point is the mechanical pivot point for the needle,

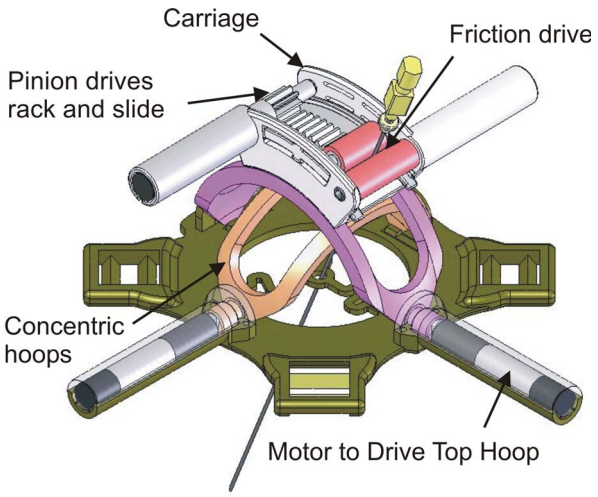


**Fig. 4 Robopsy's spherical mechanism. Concentric nested hoops allow for orientation of the needle in two compound angles. The hoops are actuated using microgear motors. The carriage riding in the two hoops performs the needle gripping and insertion.**

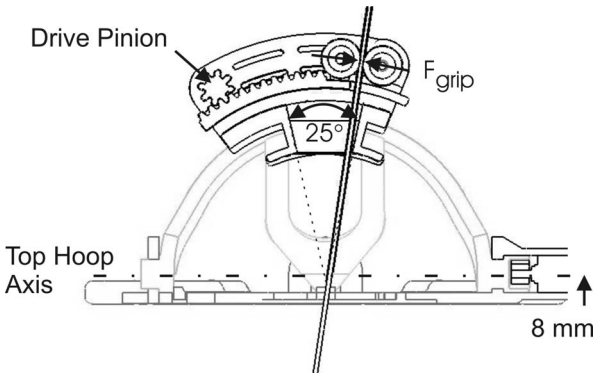


**Fig. 5 Section view of Robopsy. A pinion, actuated by a motor, drives a rack that applies a perpendicular gripping force to the needle. When released, the needle is free to "waggle" within a 25 deg cone.**

which in the current prototype is located only 8 mm above the skin surface. The base was sized with an outer diameter of 100 mm so that it is large enough to yield a structure sufficiently strong to impart the necessary insertion force to the needle and provide surface for mounting enough adhesive to obtain a stable footing, while fitting on the curved thorax of the patient. Further customization of the base is possible to fit specific regions of the body. Both hoops are slit in the middle so as to provide a double track in which a carriage, contained within both slots, rides so that it can be positioned within a hemispherical workspace via the hoops' motions. This describes the needle's compound angle.

The carriage riding in the two hoops provides for the two remaining DOFs: on-command needle gripping and needle insertion. Various methods of coupling insertion and gripping motion were explored via mechanisms such as those found in propelling pencils, drill chucks, and screw extruders. The most effective solution was to employ a friction drive in the form of two rollers, with one powered and the other freewheeling, which grip the needle. When the rollers are fully separated, a needle is free to move within the necessary 25 deg cone, which forms a waggle window, thus fulfilling the requirement that the needle not be rigidly held while resting inside the lung. This space, when the rollers are separated, also allows the device to be removed independent of the needle, so that the patient can be instantly bandaged upon needle removal or in the unlikely case that the doctor wishes to regain full manual control.

It was initially thought that both rollers needed to move inward, so as to grip the needle; however, moving the powered roller and corresponding motor would have added an unnecessary degree of complexity. Instead, the passive roller is fixed to the slide, which runs in a slot in the carriage, and the drive roller is fixed to the carriage structure. As shown in Fig. 5, the slide is driven by means of an integrally molded rack and motor-actuated pinion affixed to the carriage. The slide has a curvature concentric to that of the top hoop so that the griping force from the rollers does not tend to misalign the needle. Beginning with the needle somewhere within the 25 deg waggle window, the needle is pushed to the side against the powered roller as the slide closes. Simultaneously, the bottom hoop moves 12.5 deg in the opposite direction to the slide, effectively maintaining the desired center position of the needle, so that it is driven straight along the set compound angle. The slide is equipped with a scalloped guide, which centers the needle between the two rollers, thus handling alignment in the other direction.

Following the principles of Design for Manufacture and Assembly [19], all components were engineered for mass production via injection molding and snap-fit assembly. Currently, the prototypes are 3D printed by stereolithography (SLA) in a resin, by Vaupell Rapid Solutions (Hudson, NH). The SLA rapid prototype required minimal finish work, only light sanding on some of the pivot points. During assembly, the two hoops are first aligned and the carriage is pushed through, and then the bottom hoop is rotated 90 deg to snap into its operational position. Next the hoops are slightly compressed and snapped between the mating tabs of the base. The slide's passive roller is assembled and slid into its track in the carriage. The pinion is pushed through the motor socket, which is of larger diameter than the opposing bearing bore, and the motor, in turn, secures the pinion. The four microgear motors are fitted with v-shaped metal couplings that mate with matching grooves in the driven plastic components. Finally, the rubber coated drive roller is slid into place. Each device is designed to be used only once so no bearings are employed; all rotary joints are of the pin-in-hole form. The base is equipped with tabs for taping and slots for securing straps if required. Currently, various foam-backed medical grade adhesives are being tested. The adhesive is cut in the shape of a ring, matching the device base, with four projecting tabs for pulling tight during affixation. This has performed well during testing and can be seen in Fig. 11(*B*). The only specialized work is the application of rubber to the drive roller and the laser welding of the couplings onto the 2 mm gear head shafts, but more economical options are being explored.

**3.2 Structural Design and Analysis.** Static finite element analysis of the structure was carried out using COSMOSWORKS 2004 (SolidWorks Corp., Santa Monica, CA) to ensure that the plastic components could withstand the forces and moments due to the needle orientation and insertion. The material properties of the SLA 14120 photopolymer resin were obtained from Vaupell and a linear elastic model with a Young's modulus of 2.46 GPa and ultimate tensile strength of 45.7 MPa was used. These properties are similar to those of ABS and nylon and this is conservative, as the final medical grade plastic will be stronger and more durable. Each component was analyzed separately and the loads and boundary conditions applied were based on calculated interaction forces and constraints between the parts. For example, in modeling the loading of the hoops and base, a worst case scenario of 10 N insertion force applied solely to the middle of the lower hoop was assumed.

Hertz contact stress analysis was used in the design of the friction drive to ensure that the contact stresses between the needle and the rollers were not excessive. Rubber was bonded onto the drive roller to decrease the contact stress and improve traction.

**Table 1 Advantages and disadvantages of various actuation strategies**

| Actuation strategy | Advantage | Disadvantage |
|---|---|---|
| Pneumatic | Clean, CT compliant | Difficult to control |
| Hydraulic | CT compliant | Fluid leakage, messy, stiff hoses |
| Cable driven | CT compliant | Pulleys required for efficient cable routing |
| Flexible shaft | CT compliant | Cable windup, stiff cables |
| Micromotor | Clean, flexible cables, precise, compact | Not CT compliant if the motors are positioned in the scan plane |

This also increased the coefficient of friction between the needle and roller, thus decreasing the required griping force, as well as increasing the contact area so as to reduce the maximum contact stress on the roller.

**3.3 Actuator Selection for CT Compatibility.** A number of different strategies were considered to actuate the mechanism and some of the advantages and disadvantages of each are shown in Table 1. Micromotors with planetary gear heads where chosen due to their compact, lightweight package, and off-the-shelf availability.

As aforementioned, in order to not obscure the desirable needle artifact, and preclude generating additional artifacts, the device is made primarily from plastic. The micromotors and gear boxes, which have the potential to generate significant image-obscuring artifacts, are positioned so that when the device is located over the desired insertion point and rotated so that the tabs align with the patient's axes, a clear scan plane free of any metallic elements is provided, as shown in Fig. 6. This method of positioning artifact generating materials outside the scan plane is common practice in patients with surgical implants. Generally, when the needle is tilted, the gantry is tilted concurrently so as to keep the needle in the scan plane, thus the carriage's motors remain outside the scan plane.

**3.4 Torque Budgets.** In order to size and select the microgear motors, it was necessary to estimate the torque required to actuate each DOF of the device. This was done based on simple first order calculations (illustrated in Fig. 7) and using the data obtained from the bench level experimentation.

As discussed previously, a friction drive was chosen for needle gripping and insertion and the maximum insertion force, $F_{\text{insertion}}$, was estimated to be 10 N. From Eq. (1), for a specified insertion force, the torque required for a friction drive, $\tau_{\text{drive roller}}$, is proportional to the radius of the roller, $r_{\text{driver roller}}$. A roller diameter of 10 mm was chosen, resulting in a torque requirement of 50 N mm for the friction drive. In order to supply 10 N of drive force to the needle without slipping, a sufficiently large gripping force is required, determined by the specified insertion force and coefficient of friction between the rollers and the needle, $\mu_{\text{roller}}$. In the initial torque budget for the motors, a friction coefficient of 0.25 between the rollers and the needle was assumed, giving a required gripping force, $F_{\text{grip}}$, of 40 N calculated from Eq. (2).

$$\tau_{\text{drive roller}} = F_{\text{insertion}} \times r_{\text{driver roller}} \tag{1}$$

$$F_{\text{grip}} = F_{\text{insertion}}/\mu_{\text{roller}} \tag{2}$$

The torque required for the pinion to actuate the slide and grip the needle, $\tau_{\text{pinion}}$, is calculated from Eq. (3) and is proportional to the pinion radius, $r_{\text{pinion}}$. Reducing this radius reduces the torque required by a motor; however, minimum pinion size is a function of module. In order to provide sufficient gripping force within the given space constraints and have sufficiently strong gear teeth, while allowing smooth motion, a module of 1 mm and a pressure angle of 20 deg were selected for the 10 mm wide pinion and gear

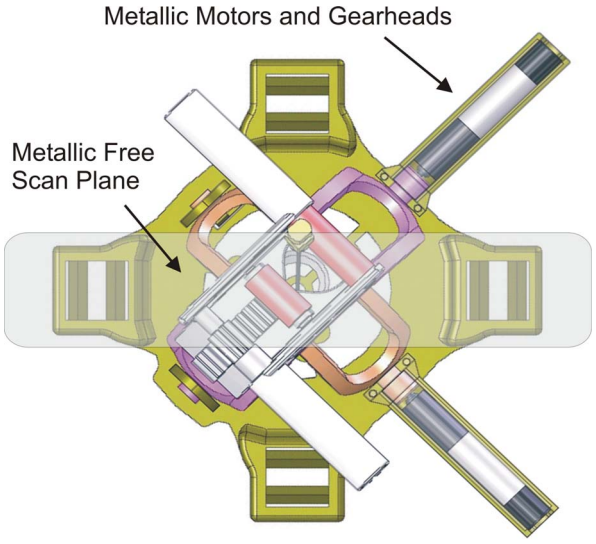


**Fig. 6 Scan transparency. The motors are placed so there is a metal-free zone where the needle is gripped and scanned. This ensures that Robopsy creates minimal distorting artifacts in the CT scan image.**

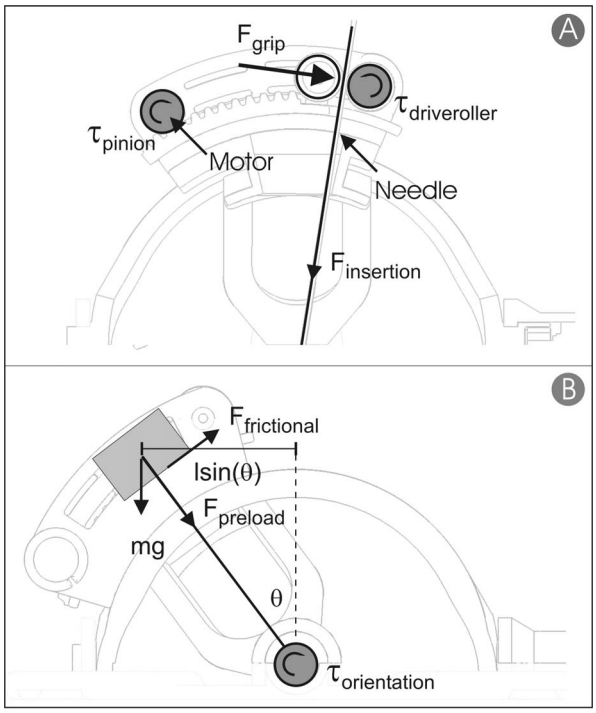


**Fig. 7 Estimating the loads required for motors to insert and orientate a needle**

rack. This yielded a torque requirement of 160 N mm and the desired pinion gearmotor's torque was thus conservatively determined to be 200 N mm.

$$\tau_{\text{pinion}} = F_{\text{grip}} \times r_{\text{pinion}} \tag{3}$$

The torque required to orientate the needle, $\tau_{\text{orientation}}$, is estimated by a summation of three components: the torque to position the carriage against gravity, $\tau_{\text{mass}}$, the torque to overcome sliding friction between hoops and carriage and bearing surfaces, $\tau_{\text{friction}}$, and the torque required to manipulate the needle, $\tau_{\text{needle}}$, which depends on the current insertion depth (obtained from bench level experiments). The mechanism was designed to provide a maximum angular displacement, $\theta$, of 30 deg off center; thus with the ~100 g carriage mass, $m$, in this position and using an average hoop radius of 50 mm, the torque required to support the mass when tilted is estimated as 30 N mm from Eq. (4). Based on a coefficient of friction for sliding nonlubricated plastic parts, $\mu_{\text{plastic}}$, of 0.25 and a preload of 0.6 N, the frictional torque was estimated to be 20 N mm from Eq. (5). Finally, adding to this the empirically determined 50 N mm torque required to orient the needle when inserted into tissue, the total torque necessary to orient the hoops, $\tau_{\text{orientation}}$, was estimated at 100 N mm from Eq. (6).

$$\tau_{\text{mass}} = mgl \sin(\theta) \tag{4}$$

$$\tau_{\text{frictional}} = (mg + \text{preload})\mu l \tag{5}$$

$$\tau_{\text{orientation}} = \tau_{\text{mass}} + \tau_{\text{frictional}} + \tau_{\text{needle}} \tag{6}$$

**3.5 Actuation and Control Implementation.** To stay within the desired form factor and keep the pivot point as near the skin as possible, 10 mm diameter brushed dc servomotors with 256:1 planetary gear boxes, model 10/1, were selected (MicroMo Electronics Inc. (Faulhaber Group), Clearwater, FL). Together they are rated for a peak intermittent torque of 200 N mm, which fulfills the design specifications and allows needle orientation at a speed of 360 deg/s, a gripping time of 1 s, and an insertion speed of 20 mm/s. Encoders were fitted on the rear shaft of the motors to enable closed loop servo control. While the hoops and friction drive's roller are operated under position control, the gripping axis is operated by commanding an overshot position and then controlling current so as to modulate the gripping force. The controller and motor amplifier boards are from Galil Motion Control (Rocklin, CA). Galil's Ethernet motion controllers are designed for cost and space sensitive applications. A four axis controller board, model DMC2143, is used with a brushed dc motor amplifier, model AMP20341, and a compact 65 W power supply providing 24 V and ±12 V. The controller is communicated with over TCP/IP, using either a LAN or crossover cable, via a proprietary Active-X toolbox supplied by Galil. The Robopsy graphical user interface is written in VISUAL BASIC 6.

The motor wiring and electronics installation were designed to maximize flexibility and make the system modular. The electronics are housed in an enclosure, which rests on a cart next to the patient and connects to a 120 V wall outlet. An Ethernet cable for communication connects to the computer running the interface in the control room and an ultra flexible cable connects to the actuation module positioned on the patient on the CT scanner bed. The enclosure was customized with laser cutting and standard machining and is fitted with power switches and a cooling fan. The Ethernet cable travels under the door of the scanner room, or through a port in the wall, into the control room where it connects to a laptop running the custom VISUAL BASIC interface. This way the device is driven remotely from the radiation shielded control room. Each of the four axes requires six conductors, two for the motor and four for the encoder.

Traveling from the control box to the patient is a single 12 ft, 27-conductor ultra flexible cable (Cooner Wire Inc., Chatsworth, CA), which terminates in a D-sub connector. The mating connector of the actuation module is equipped with four 1 ft, six-conductor, ultra flexible cables soldered to each motor and encoder, which are secured to the device structure and looped so as to permit motion and minimize parasitic torques. This way the device can be easily connected and disconnected postprocedure. The entire system, shown in Fig. 8, fits into a small suitcase and is easy to transport and position.

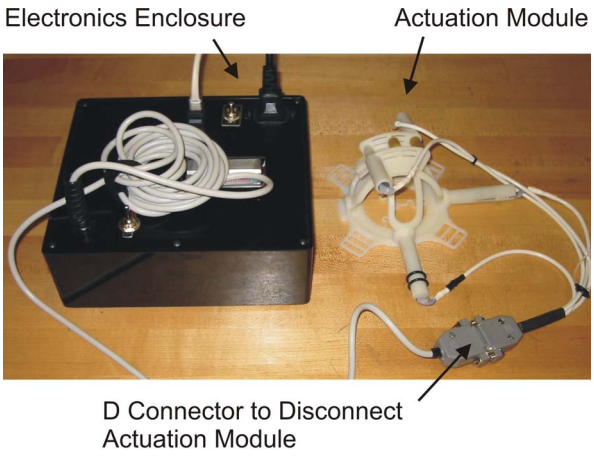


**Fig. 8 Robopsy prototype. The actuation module is connected to the electronics enclosure using a flexible cable and a D-sub connector. The mating D-sub then connects via four pigtails to each motor.**

## 4 Device Validation and Testing

Testing of the system has been performed in conjunction with a Siemens Somatom Sensation 64 CT (Siemens Medical Solutions, Erlangen, Germany) in order to evaluate CT compatibility and validate the system operation. We have demonstrated the function of the double hoop orientation mechanism and the needle griping and insertion mechanism using thoracic phantoms. A protocol for animal testing has been approved by the MGH Subcommittee for Research Animal Care, and animal testing is currently on-going.

**4.1 Insertion Capability.** Various coatings on the rollers were tested in order to optimize needle insertion. In particular, 1 mm thick surgical tubing, 0.5 mm thick high grip neoprene, and 0.75 mm thick heat shrink were assessed to determine, which yielded the best needle insertion force and minimized slipping. A needle was loaded into the top of the device and gripped with an approximate force of 40 N. A spring scale was attached to the top of the needle and the device pulled downward until the needle slipped. The results are summarized in Table 2.

The best performing material was the 1 mm thick surgical tubing, slightly stretched over the plastic rollers, which yielded an insertion force of 8.6 N with a 16 gauge (1.6 mm) polished stainless steel needle. However, the design specifications called for 10 N of insertion force. For the surgical tubing and heat shrink tubing, the maximum insertion force was found to decrease with needle diameter; this occurs with the thicker coatings because of their compliance. When the needle diameter becomes completely

**Table 2 Friction drive insertion force testing**

| Material | Max force (N) (1.17 mm needle) | Max force (N) (1.62 mm needle) |
|---|---|---|
| Surgical tubing | 4.9 | 8.6 |
| High grip neoprene | 6.3 | 3.4 |
| Heat shrink | 2.9 | 4.9 |

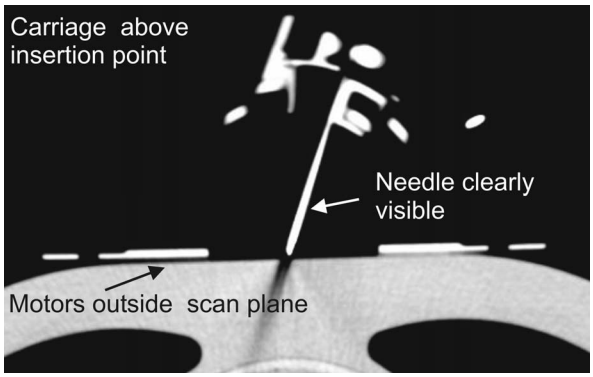


**Fig. 9 CT Compatibility. CT scan showing that the hoops' motors lie outside of the scan plane when the hoops are orientated at 45 deg with respect to the scan plane. This ensures that Robopsy creates minimal artifacts in the CT scan.**

enveloped, the rollers begin to exert a force directly on each other, thus reducing the griping force applied to the needle.

**4.2 Phantom Experiments.** Initial testing of Robopsy was performed on thoracic phantoms to verify CT compatibility and the ability to successfully target lesions remotely using the device.

*4.2.1 CT-Compatibility Validation*. Testing of the device on a thoracic phantom confirmed that it can be successfully operated remotely while in the CT bore. In Fig. 9, it can be seen that the metallic motors lie sufficiently outside the scan plane so as to minimize metallic beam-hardening artifacts. Indeed, with the hoops straight up and the device rotated so that both hoops' planes are positioned at 45 deg with respect to the scan plane, the motors that actuate the hoops and carriage cannot be seen in this CT image (see Fig. 5). The carriage is only slightly visible and located approximately 50 mm above the needle insertion point; thus there is a clear image of the needle and its trajectory.

*4.2.2 Gelatin Phantom Targeting Experiments*. Early targeting trials were performed on a uniform and sanitary custom thoracic phantom comprised of ballistic gelatin shown in Fig. 10(*A*), which has a consistency similar to human tissue and is used for ordnance testing (Vyse Gelatin Company, Schiller Park, IL). Target lung nodules were simulated by glass beads, ranging in size from 2 mm to 20 mm, cast into the gelatine below plastic piping that mimicked ribs around which the needle was to steered. This phantom was positioned on the CT bed, as a patient would be, and the standard biopsy procedure performed remotely from the control room by a trained interventional radiologist. The resulting image from one of the phantom experiments is shown in Fig. 10(*B*), clearly demonstrating the center of a lesion being successfully targeted.

Preliminary testing with the phantom indicated that Robopsy could successfully remotely target a lesion in reduced time and with reduced radiation dose, compared to the manual procedure. A broader study to establish a concrete base line for the manual procedure is currently underway.

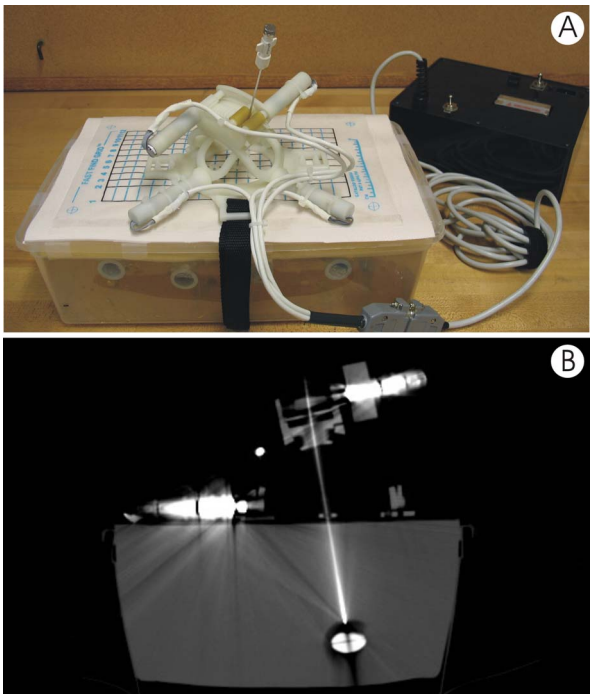


**Fig. 10 Phantom targeting experiments. (*A*) Robopsy placed over the metallic grid on the custom made phantom. (*B*) CT scan showing Robopsy being used to target a lesion. Robopsy was used to align the needle with the CT gantry so that the needle is fully visible.**

**4.3 Initial in Vivo Porcine Study.** Initial in vivo validation in a quietly sedated respiring pig was conducted with positive results. Key images from the first porcine test are shown in Figs. 11 and 12.

*4.3.1 Lesion Creation*. Prior to performing the Robopsy assisted biopsy, it was necessary to create simulated, radio-dense lesions in the lung parenchyma. A solution of agros, which thickens and hardens shortly after being prepared, was mixed with 37% iodine contrast agent for visibility. This was sufficiently inviscid that it could be injected in a metered manner with a 22 gauge (0.644 mm) needle. The pig was anesthetized, incubated, connected to a respirator to maintain lung inflation, and placed on the CT bed in the head-first, left decubitus position (i.e., lying on its left side with head pointing into the scanner bore). A standard positioning grid was affixed and a detailed scan of the thorax was

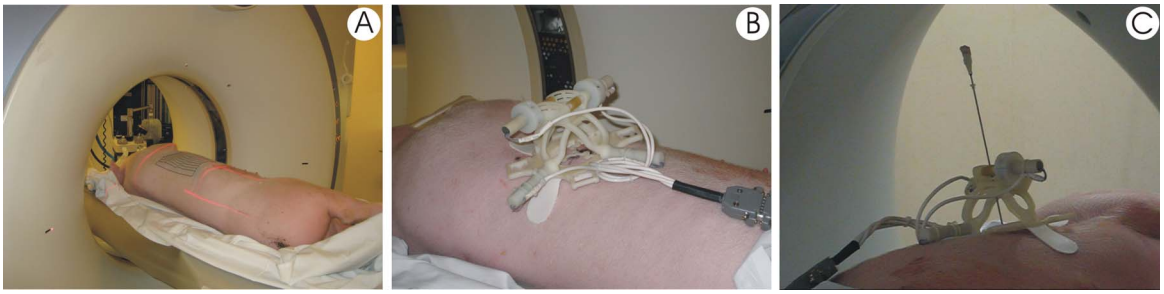


**Fig. 11 Porcine testing. (*A*) Pig in scanner with targeting grid applied. (*B*) Device adhesive mounted to pig. (*C*) Needle orientation and insertion conducted remotely inside scanner.**

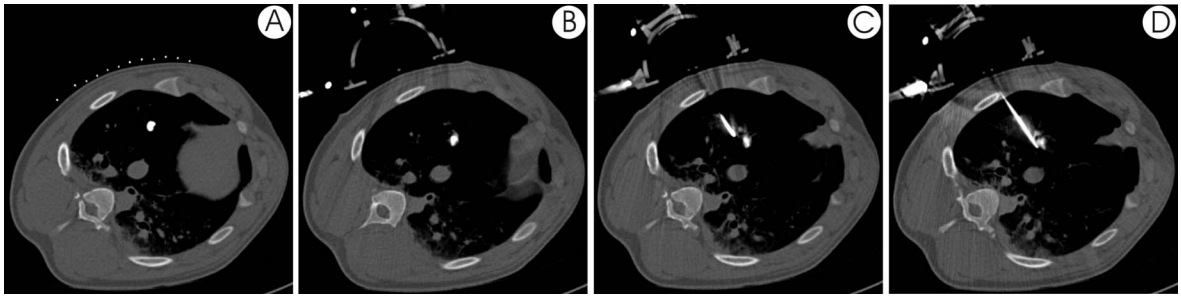


**Fig. 12 Four CT scans from the initial in vivo porcine trial. (*A*) Lesion injected; (*B*) device affixed; (*C*) nearly at lesion; (*D*) lesion targeted.**

acquired. From this scan, three locations and insertion trajectories inside the right lung were selected for lesion creation. Using the grid, the selected insertion points were marked on the pig's chest. Then, moving a little to the side of these marks, three artificial lesions were injected into the lung. During injection, the needle was released while in the lung and observed to oscillate in a 10 deg arc, thus demonstrating the importance of allowing for a nonrigid rest position for the needle.

*4.3.2 Lesion Targeting*. The biopsy procedure commenced with a scout scan, which confirmed the location of the lesions. One lesion, approximately 2 cm in diameter, was selected for targeting. The gantry table, along with the pig, was then slid out of the scanner bore. A small superficial incision was made with a scalpel at the selected needle entry point. The device was affixed over the incision via the 3M foam-backed medical grade adhesive (3M, St. Paul, MN), which, even when applied directly over the bristle without shaving, yielded a secure placement with the device resisting both lateral and vertical displacements. Postprocedure, the device was easily peeled off with minimal tugging of the skin. The affixed device was observed to rise and fall approximately 2 cm with respiration, thus demonstrating the benefit of patient mounting.

The Robopsy interface was activated, the pig returned to the scanner bore, and the needle gripped. A second scan was conducted and the angles from the needle tip to lesion were measured as well as the depth, along this line to the lesion. Then using the custom interface, the needle was oriented to the measured angles and inserted to the measured depth. The third scan indicated that only a small correction of 3 deg and a further needle insertion of 4 mm were needed. The fourth and final scan confirmed that the needle had successfully targeted the simulated lung nodule as can be seen in Fig. 12(*D*). As the needle hit the nodule, it was deflected to the side due to the agros' solidity.

This first porcine trial demonstrated the ability, after applying the device, to successfully target a lesion remotely, guided by CT images. Time was not measured, but during upcoming porcine trials is expected to be significantly reduced. Targeting was accomplished with the expected minimum of four scans: one for insertion point selection and trajectory planning, one to register the device to the pig and accomplish insertion to the pleura, one for fine adjustment and final insertion, and the final to confirm needle tip placement in the lesion. These four scans are shown in Fig. 12. In an observational study of ten consecutive manual lung biopsies, approximately a dozen scans were needed to reach the target (unpublished results). These results underscore the potential for procedural time and dose reduction and increased efficiency through the use of a telerobotic needle orientation and insertion device.

## 5 Conclusions and Future Work

The tests conducted indicate that Robopsy can significantly improve an interventional radiologist's ability to target a thoracic lesion by enabling fuller utilization of the CT scanner's precise positional data. A Robopsy-based biopsy can reduce procedure time and radiation dose, permit the operator to target smaller lesions and specific regions within a lesion more consistently, and decrease the average number of needle insertions through the chest wall and pleura. This will reduce patient complications and increase CT scanner availability for other tasks. The lung biopsy procedure was chosen initially due to the complications that arise due to the patient respiration, making it one of the more difficult biopsy procedures to perform. Similar image-guided targeting is necessary in other biopsy procedures, targeted ablations, brachytherapy seed implantations, and other image-guided percutaneous interventions. With minimal modification, the prototype Robopsy system can be adapted for and extended to cover these and many other applications.

The next step is to undertake a final evolution of the design so the components can be injection molded, which will remove the backlash present in the rapid prototyped parts. With the new design implementation, more extensive porcine tests will be done, which then will lead to human trials.

## Acknowledgment

The authors would like to thank the Center for Integration of Medicine and Innovative Technology (CIMIT) for providing funding for this work from U.S. Army Medical Acquisition Activity (USAMRAA) under cooperative Agreement No. DAMD 17-02-2-0006 and for MGH for providing the use of the CT facilities. In addition, the MIT IDEAS Competition, MIT $100K Competition and the NCIIA BMEidea competition have provided strategic and financial assistance to the project. The project began in MIT course 2.75 *Precision Machine Design* taught by Professor Alexander Slocum and the authors wish to acknowledge student design team member Steven Barrett for his contribution to the initial research, concept generation, analysis, and testing. Special thanks also to Professor Bernie Roth for his input on the background of spherical mechanisms.

## References

[1] American Lung Association, 2006, "Trends in Lung Cancer Morbidity and Mortality," Epidemiology and Statistics Unit.
[2] Henschke, C. I., Yankelevitz, D. F., Altorki, N. K., et al., 2006, "Survival of Patients with Stage I Lung Cancer Detected on CT Screening," N. Engl. J. Med., **355**(17), pp. 1763–1771.
[3] Ohno, Y., Hatabu, H., et al., 2003, "CT-Guided Transthoracic Needle Aspiration Biopsy of Small (⇐20 mm) Solitary Pulmonary Nodules," AJR, Am. J. Roentgenol., **180**(6), pp. 1665–1669.
[4] Brabrand, K., Aaløkken, T. M., Krombach, G. A., Günther, R. W., Tariq, R., Magnusson, A., and Lindgren, P. G., 2004, "Multicenter Evaluation of a New Laser Guidance System for Computed Tomography Intervention," Acta Radiol., **45**(3), pp. 308–312.
[5] LAP of America L.C., 1755 Avenida del Sol, Boca Raton, FL 33432, http://www.lap-laser.com/
[6] Rasmus, M., Dziergwa, S., Haas, T., Madoerin, P., Huegli, R., Bilecen, D., and Jacob, A. L., 2007, "Preliminary Clinical Results with the MRI-Compatible Guiding System INNOMOTION," Int J CARS, **2**, pp. S138–S145.
[7] Stoianovici, D., Cleary, K., Patriciu, A., Mazilu, D., Stanimir, A., Craciunoiu, N., Watson, V., and Kavoussi, L., 2003, "AcuBot: A Robot for Radiological Interventions," IEEE Trans. Rob. Autom., **19**(5), pp. 927–930.

[8] Cleary, K., Stoianovici, D., Patriciu, A., Mazilu, D., Lindisch, D., and Watson, V., 2002, "Robotically Assisted Nerve and Facet Blocks: A Cadaveric Study," Acad. Radiol., **9**, pp. 821–825.
[9] Cleary, K., Zigmund, B., Banovac, F., White, C., and Stoianovic, D., 2005, "Robotically Assisted Lung Biopsy Under CT Fluoroscopy: Lung Cancer Screening and Phantom Study," Computer Assisted Radiology and Surgery: Int. Cong. Series, **1281**, pp. 740–745.
[10] Maurin, B., Bayle, B., Gangloff, J., Zanne, P., de Mathelin, M., and Piccin, O., 2006, "A Robotized Positioning Platform Guided by Computed Tomography: Practical Issues and Evaluation," *Proceedings of IEEE 2006 International Conference on Robotics and Automation*, Orlando, Fl, pp. 251–256.
[11] Taillant, E., Avila-Vilchis, J. C., Allegrini, I. B., and Cinquin, P., 2004, "CT and MR Compatible Light Puncture Robot: Architectural Design and First Experiments," *Proceedings of 2004 International Society and Conference Series on Medical Image Computing and Computer-Assisted Intervention*, Vol. 2, pp. 145–154.
[12] Muntener, M., Patriciu, A., Petrisor, D., Mazilu, D., Bagga, H., Kavoussi, L., Cleary, K., Stoianovici, D., 2006, "Magnetic Resonance Imaging Compatible Robotic System for Fully Automated Brachytherapy Seed Placement," Urology, **68**(6), pp. 1313–1317.
[13] Patriciu, A., Petrisor, D., Muntener, M., Mazlie, D., Schar, M., and Stoianovici, D., 2007, "Automatic Brachytherapy Seed Placement Under MRI Guidance," IEEE Trans. Biomed. Eng., **54**(8), pp. 1499–1506.
[14] Barrett, J. F., and Keat, N., 2004, "Artifacts in CT: Recognition and Avoidance," Radiographics, **24**, pp. 1679–1691.
[15] Okanura, A. M., Simone, C., and O'Leary, M. D., 2004, "Force Modeling for Needle Insertion into Soft Tissue," IEEE Trans. Biomed. Eng., **51**(10), pp. 1707–1716.
[16] Dien, R. Y., and Luce, E. C., 1986, "Spherical Robotic Wrist Joint," U.S. Patent, 4,628,765, Rensselaer Polytechnic Institute.
[17] Stanisic, M., Duta, O., 1990, "Symetrically Actuated Double Pointing Systems: The Basis of Singularity-Free Robot Wrists," IEEE Trans. Rob. Autom., **6**(5), pp. 562–569.
[18] Rosheim, M., 1989, "Wrist Tendon Actuator," U.S. Patent, 4,804,220.
[19] Boothroyd, G., Dewhurst, P., Knight, W., 2002, *Product Design for Manufacture and Assembly*, 2nd ed., Dekker, New York.